European Journal of Neuroscience, Vol. 24, pp. 1664–1674, 2006 doi:10.1111/j.1460-9568.2006.05053.x

Nyctalopin is essential for synaptic transmission in the cone dominated zebrafish retina

Ronja Bahadori,[1]* Oliver Biehlmaier,[1,2]* Christina Zeitz,[3]* Thomas Labhart,[2] Yuri V. Makhankov,[1] Ursula Forster,[3] Matthias Gesemann,[1] Wolfgang Berger[3] and Stephan C. F. Neuhauss[1,2]
[1]Swiss Federal Institute of Technology (ETH) Zurich, Department of Biology, and the Brain Research Institute, at the University Zurich, Zurich, Switzerland
[2]Institute of Zoology, Winterthurerstrasse 190, CH 8057 Zurich, Switzerland
[3]Division of Medical Molecular Genetics and Gene Diagnostics, Institute of Medical Genetics, University of Zurich, Zurich, Switzerland

Keywords: bipolar cell, cone photoreceptor, electroretinogram, nyctalopin, photoreceptor synapse, retina

Abstract

The first synapse in the vertebrate visual system is the photoreceptor synapse between rod and cone photoreceptors and the second-order bipolar cells. Although mutations in the nyctalopin gene (*NYX*) in humans lead to congenital stationary night blindness (CSNB1), affecting synaptic transmission between both types of photoreceptors and ON-bipolar cells, the function of nyctalopin in cone-dominant animal models has not been studied. Because the larval zebrafish retina is cone-dominant, we isolated the zebrafish *nyx* ortholog and raised a polyclonal antibody against the protein. Nyctalopin is expressed postsynaptically in both synaptic layers of the retina. Functional disruption via morpholino antisense injection leads to characteristic defects in the electroretinogram and defects in visual contrast sensitivity. We therefore demonstrated that nyctalopin plays a similar role in retinal synapse function in the cone pathway as in the rod pathway, thereby creating a genetic model for CSNB1 and its effects on cone vision.

Introduction

The visual pathway in vertebrates is separated into ON- and OFF-center channels. ON channels respond to light onset with depolarization and offset with hyperpolarization. The reverse is true for OFF-channels. This separation already takes place in the first synapse of the visual system, where photoreceptors synapse onto bipolar cells that either hyperpolarize (ON-type) or depolarize (OFF-type) upon glutamate binding (Rodieck, 1998). This response is thought to be mediated by different neurotransmitter receptors of the metabotropic and AMPA/kainate type, respectively. In teleosts there is evidence that signals to cone ON-bipolar cells mainly involve excitatory amino acid transporters (Grant & Dowling, 1995; Wong et al., 2005).

Congential stationary nightblindness (CSNB) is a family of non-progressive retinal disorders characterized by impaired night vision and myopia. These disorders are thought to be caused by defective synaptic transmisson from photoreceptors to ON-bipolar cells. Because patients are nightblind, the mutations affect mainly the scotopic (low-light vision) rod photoreceptor system. The clinical similar forms of autosomal and X-linked recessive forms of CSNB are caused by mutations in *GRM6* encoding the metabotropic glutamate receptor (mGluR6) (Dryja *et al*., 2005; Zeitz, 2005) or in *NYX* encoding nyctalopin (Bech-Hansen *et al*., 2000; Pusch *et al*., 2000), respectively.

In contrast to GRM6, the function of NYX remains to be elucidated. The *NYX* gene in human and mouse is composed of three exons and is a unique member of the small leucine-rich repeat proteoglycan family. This protein contains 11 typical leucine-rich repeats (LRRs) flanked by N- and C-terminal cysteine-rich LRRs. The LRR motif confers an ideal conformation for binding to other proteins and is therefore believed to mediate protein–protein interactions (Kobe & Deisenhofer, 1994). In humans the predicted polypeptide contains an N-terminal endoplasmic reticulum signal peptide and is glycosylphosphatidylinositol (GPI) anchored (Bech-Hansen *et al*., 2000; Pusch *et al*., 2000). Interestingly the membrane attachment of nyctalopin is species-specific with mouse nyctalopin lacking a GPI anchor and instead having a putative transmembrane domain at its carboxy terminus (Zeitz *et al*., 2003; O'Connor *et al*., 2005). In both cases the protein is extracellulary located (Zeitz *et al*., 2003). Gregg *et al*. (2003) described a mouse model *nob* (*no b-wave*) that resembles CSNB1. The strain was originally identified, based on changes in the electroretinogram (ERG). In those mice the ERG b-wave is absent, although the a-wave is normal. The CSNB-typic shape of the ERG response suggests a defect in synaptic transmission between photoreceptor and ON bipolar cells (Pardue *et al*., 1998).

In the mouse, the expression of *Nyx* was found in all retinal cell layers and was most abundant in cells of the inner nuclear layer (INL), where bipolar cell bodies are located (Gregg *et al*., 2003). Other studies found expression in the INL and the ganglion cell layer with protein localization in these cell layers and the inner and outer synaptic layers (Pesch *et al*., 2003; Ren *et al*., 2004). In the human retina *NYX* expression has been reported in all synaptic layers, including the photoreceptor cell layer (Bech-Hansen *et al*., 2000). Hence, the expression pattern of the gene is still controversial or might be different in various vertebrate species.

Correspondence: Dr S. Neuhauss, [2]Institute of Zoology, as above.
E-mail: stephan.neuhauss@zool.unizh.ch

*R.B., O.B. and C.Z. contributed equally to this work.

Received 15 November 2005, revised 6 July 2006, accepted 19 July 2006

In order to investigate the function of nyctalopin in cone-driven vision, we studied this gene in zebrafish. The larval zebrafish retina develops rapidly and is functionally cone driven (Clark, 1981; Bilotta *et al*., 2001). Owing to its superb genetics, the zebrafish is well suited to study cone vision by genetic means.

We therefore cloned the zebafish (zf) *nyx* ortholog and raised a polypeptide antibody to study both its expression pattern and protein localization. We localized the protein postynaptically in both synaptic layers. Loss of function induced by morpholino antisense injection revealed a defect in synaptic transmission of the ON-pathway and impaired contrast sensitivity in visual performance assays.

Materials and methods

Fish maintenance and breeding

Experiments were carried out in accordance with the European Communities Council Directive for animal use in science (86/609/EEC). Wild-type fish from the inbred WIK strain were used throughout the study. They were bred and crossed as previously described (Brand & Nüsslein-Volhard, 2002). Embryos were raised at 28 °C in E3 medium (5 mM NaCl, 0.17 mM KCl, 0.33 mM $CaCl_2$ and 0.33 mM $MgSO_4$) and staged according to development in days post-fertilization (dpf).

Isolation of the zebrafish (zf) nyx cDNA

The human *NYX* cDNA sequence (accession no. NM022567) was analysed for orthologous sequences by the Blast program of the Ensemble genome data resources. The obtained sequence information was used to design oligonucleotides (*Nyx*zebrafFOR: 5′-GCACATGCACTCAGGAGAAG-3′ and *Nyx*zebrafREV: 5′-CGATTCTCTTGCAAGTTGAGG-3′) for PCR amplification of a zf *nyx* probe (550 bp), corresponding to exon 3 of the human *NYX* gene. A high-density filter of a zebrafish retina cDNA library (Library No. 760; Resource Centre/Primary Database, Berlin, Germany) was hybridized with the ^{32}P-dCTP-labelled probe to obtain the complete open reading frame (ORF) of the zf *nyx* gene. DNA from positive clones was isolated (Plasmid Midi Kit; Qiagen, Hombrechtikon, Switzerland) and insert size was determined by digestion with restriction enzymes *Sac*I and *Kpn*I. One of the positive clones was entirely sequenced with standard M13 forward (5′-GTTTTCCCAGTCACGACG-3′) and reverse (5′-CAGGAAACAGCTATGACC-3′) primers.

Computational analysis of the zebrafish nyx sequence

The *nyx* zebrafish cDNA sequence was applied to different computational programs. To obtain the exon–intron boundaries, the cDNA sequence was aligned to genomic *Danio rerio* sequences from the Ensemble genome data resources (see above) or to the whole shotgun sequence data available at the NCBI. Putative protein motifs (signal sequence, LRRs and GPI anchor) were predicted with the most recent (May 2005) Expasy Proteomics tools available at http://www.expasy.org/tools/. The sequence alignment was performed with PRETTY from GCG.

RNA probe and whole mount in situ hybridization

As a template, a 1000-bp PCR fragment of the zf *nyx* was amplified by using a forward primer *Nyx-fw* (GGCTTGCACACGCTCCT) and reverse Primer *Nyx-rev* (AGTCTGAGAAGCACCGAACA) and subcloned into the cloning vectors (TOPO PCR II or TOPO PCR 2.1 vectors, Invitrogene, Basel, Switzerland). Two micrograms of the linearized plasmid was *in vitro* transcribed by using the digoxigenin labeling kit (Roche, Switzerland). The antisense and sense RNA probes were synthesized with the T7 RNA polymerase and Sp6 RNA polymerase, respectively.

To prevent melanization, the zebrafish larvae were treated with 1-phenyl-2-thiurea (Sigma, Saint Louis, MO, USA) and fixed after being anaesthetized on ice at different stages in 4% paraformaldehyde (4% in PBS, pH 7.2). Whole mount *in situ* hybridization was performed as previously described (Thisse *et al*., 1993). Fixed larvae were cryoprotected in 30% sucrose for at least 2 h. Whole larvae were embedded in Cryomatrix (Jung-Leica; Tissue Freezing Medium), rapidly frozen in liquid N_2; 30-μm-thick sections were cut at −20 °C, mounted on SuperFrost Plus slides, air dried at 37 °C for at least 2 h, washed in 1× PBS pH 7.4 and mounted.

Expression construct and transfection

The expression construct was generated by using the mammalian pcDNAI-SS-Flag vector (Invitrogen). The zebrafish *nyx* insert was amplified with a DNA polymerase kit containing a proofreading activity (ProofStart, Qiagen), Q-solution and 1.5 mM $MgCl_2$ with gene-specific primers (For: 5′-AAAAGAATTCTGGGCTTGCACACGCTC-3′; Rev: 5′-AAAAAAAAGCGGCCGCTCAAGAGGCATTAATGGAGT-3′) at an annealing temperature of 62 °C. The positive cDNA clone from above was used as the template. The product was subcloned in a shuttle vector (pCR-Blunt II-TOPO, Invitrogen), and DNA from plasmids was sequenced with standard methods. The plasmid containing the correct sequence was *Eco*RI/*Not*I-digested and ligated in the mammalian expression vector treated in the same way. The day before transfection, 1×10^5 COS-7 cells were spread in a six-well device containing cover slides in MEM (Laboratory Force, Nunningen, Switzerland), containing 3 mM L-glutamine, streptomycin (100 U/mL) and penicillin (100 U/mL). Transfection was performed with polyethylenamine (PEI; Fluka, Buchs, Switzerland) (NaCl/PEI = 8) and 4.8 μg DNA per well. While the DNA complexed with PEI, cells were washed with PBS and medium was replenished. After 30 min the transfection complex was added to the cells.

After 24 h incubation at 37 °C under 5% CO_2, cells were washed with PBS and fixed for 10 min in 4% formaldehyde. After three washes with PBS, cells were permeabilized with 0.2% TritonX-100 in PBS. Then, cells were incubated with preabsorbed zfanti-Nyx and anti-flag (Sigma) antibodies at a dilution of 1 : 500 in PBGT for 1 h. After three PBGT washes, cells were incubated with anti-rabbit Cy3 and anti-mouse FITC antibody, again washed three times in PBGT, fixed and then embedded in anti-fade mounting media as described previously (Zeitz *et al*., 2003).

Target gene knock down (Morpholino)

An antisense morpholino (MO; Gene-Tools, LLC) was designed against the translation site with the sequence of 5′-GAAGCCAGTGATGTGTTTCATCATCATCAATA-3′. For the control injection a standard MO 5′-CCTCTTACCTCAGTTACAATTTATA-3′ (Gene-Tools, LLC) was used. The morpholinos were dissolved in water (2 mM stock solution) and diluted to 1 mM in 0.3× Danieau's solution [1× Danieu: 58 mM NaCl, 0.7 mM KCl, 0,4 mM $MgSO_4$, 0.6 mM $Ca(NO_3)_2$, 5 mM Hepes, pH 7.6]. Approximately 15 ng and

30 ng of MO was injected into one- to eight-cell-stage zebrafish embryos in their chorions.

Histology

Paraformaldehyde-fixed larvae (4% paraformaldehyde in 0.2 M phosphate buffer, pH 7.4, for 1 h at room temperature) were dehydrated in a graded series of ethanol–water mixtures, then incubated in 1 : 1 and 1 : 3 ethanol and Technovit 7100 basic solution (Kulzer, Germany) for 1 h, respectively. After overnight infiltration in Technovit 7100 basic solution, larvae were positioned in Technovit 7100 polymerization medium overnight at room temperature.

Microtome sections (3 μm) were prepared and mounted on SuperFrost Plus slides (Menzel-Gläser), air dried at 60 °C, stained with toluidine blue solution (0.1% in distilled water), overlaid with Entellan (Merck, Darmstadt, Germany) and coverslipped.

Immunohistochemistry

To raise antibodies against zfNyx, a peptide comprising the amino acids H2N-CDS LRN GTQ QDP AESQ-CONH2 (Eurogentec S. A. Belgium) were prepared and injected into rabbits. The resulting antibody was used for zfNyx-immunostaining in wild-type and *nyx*-morphant larvae.

For immunostaining, fixed larvae were cryoprotected in 30% sucrose for at least 2 h. Whole larvae were embedded in Cryomatrix (Jung-Leica; Tissue Freezing Medium), and rapidly frozen in liquid N_2; 15-μm-thick sections were cut at −20 °C, mounted on SuperFrost Plus Slides, and air dried at 37 °C for at least 2 h. Slides were stored at −20 °C. Before further use, slides were thawed and washed in phosphate-buffered saline (PBS; 50 mM), pH 7.4, for 10 min, and treated with blocking solution [BS: 20% normal goat serum (NGS), 2% bovine serum albumin (BSA) in PBS containing 0.3% Triton X-100 (PBST)] for 1 h. Sections were then incubated overnight in primary antibody in BS at 4 °C. Rabbit anti-Nyx (1 : 500) and mouse anti-synaptic vesicle 2 (1 : 100; SV2; DSHB, Iowa, USA) or mouse anti-postsynaptic density 95 kDa (1 : 200; PSD-95; Affinity BioReagents, Golden, CO, USA), respectively, were used as primary antibodies for confocal microscopy, and the immunoreaction was visualized by using Alexa Fluor 488 anti-rabbit IgG (1 : 1000), and Alexa Fluor 568 anti-mouse IgG (1 : 500; Molecular Probes, Leiden, The Netherlands) as secondary antibodies. For all immunocytochemical experiments, negative controls were carried out in the same way but without using the first antibody. Slides were viewed with a Leica SP2 AOBS UV CLSM confocal microscope (Leica Microsystems, Glattbrugg, Switzerland). The images obtained were processed using NIH ImageJ 1.35a (National Institutes of Health, Bethesda, MD, USA) or Imaris (Bitplane, Zurich, Switzerland). Deconvolution of the Nyx/PSD-95 double-labeling was calculated by using Huygens Essential (Scientific Volume Imaging, Hilversum, The Netherlands).

Electoretinography (ERG)

Electroretinograms (ERGs) were recorded from larvae at 4 dpf as previously described (Makhankov *et al.*, 2004), with the difference that recording bandwith was from 0.1 to 100 Hz. Briefly, all specimens were dark-adapted for 30 min prior to positioning them in the recording chamber. Each larva was placed on its side on the surface of a moist sponge with E3 medium and paralysed by directly applying a droplet of the muscle relaxant Esmeron (0.8 mg/mL in larval medium; Organon Teknika, Eppelheim, Germany). Light flashes of 200-ms duration were separated by 7-s intervals. Irradiation at the position of the subject as measured by a photometer with photopic sensitivity profile was 5000 lux or 5.7 mW/cm^2. A virtual instrument under NI LabVIEW 5.1 was used both to control stimulation and to record ERG traces to a PC. Sampling was done in buffered acquisition mode with a sampling rate of 1000 Hz. Responses were averaged between three and five times depending on the signal-to-noise ratio.

Optokinetic response measurements

Behavioral contrast sensitivity was measured as described previously (Rinner *et al.*, 2005b). Briefly, to measure eye movement, single larvae were placed dorsal side up in the center of a Petridish (35 mm diameter) containing 3% prewarmed (28 °C) methylcellulose. Moving sine-wave gratings were projected by a Proxima 4200 DLP projector onto a screen within the visual field of the larva, at an apparent distance 4.65 cm from the larva's right eye. Projection size on the screen was 8 × 6 cm, subtending a visual angle of 65.6° horizontally and 53.1° vertically. Eye movements triggered by the visual stimulation were recorded by means of an infrared-sensitive CCD camera. Custom developed software on the basis of LabView IMAQ (National Instruments, version 5.1) was used to control stimulation and camera, and to analyse the resulting images.

Contrast sensitivity functions for *nyx* morphant and control-injected larvae were measured by the gain (eye velocity/grating velocity) as a function of the contrast of a moving grating. Statistics was derived as described in (Rinner *et al.*, 2005a) by bootstrap sampling of differences between randomly drawn samples ($n = 10\,000$) from a pooled data set of control and *nyx* morphants. Significance level chosen was 5% for all experiments.

Results

Several lines of evidence indicate that zebrafish larvae have a cone-dominated retina. At early stages (5 dpf) the outer retina is composed of a precisely patterned photoreceptor mosaic consisting of four cone types interspersed with rods (Branchek & Bremiller, 1984; Raymond *et al.*, 1995; Schmitt & Dowling, 1999). However, at this stage only cone photoreceptors contribute to the behavioral responses (Clark, 1981). Rods become functional only at later stages (older than 15 dpf) as determined by ERG analysis (Bilotta *et al.*, 2001). Therefore, in the following behavioral and physiological experiments, the visual responses can be regarded as derived from cone activity only.

Cloning of the zebrafish nyx ortholog

As a prerequisite to characterize the zf *nyx* gene functionally, we isolated the respective cDNA containing the complete ORF. Public database searches revealed the orthologous sequence to exon 3 of the human and mouse *NYX* gene in zebrafish, but lacked the ATG start codon. Owing to the small size of the coding region of exon 2 of the human or mouse *Nyx* gene (33 and 21 bp, respectively) database searches did not show any significant alignment with zebrafish genomic or cDNA sequences. Because 5′-RACE experiments did not provide additional sequence information (data not shown), we hybridized a zebrafish retina cDNA library with a zf *Nyx* probe (550 bp), corresponding to exon 3 of the human *NYX* gene. One of the clones (UWS_p760A1131Q2) contained the complete ORF of the zebrafish *Nyx* gene with a sequence identity of 56% to human and 53% to mouse aminoacid sequences (Fig. 1). The respective cDNA sequence has been deposited in the GenBank database (DQ201193). Interestingly, the

```
huNYX 1    MKGRGMLVLL LH↓AVVLGL.. PSAWAVGACA RACPAACACS TVERGCSVRC 48
moNyx      ~~~~~MLILL LH↓AVVFSL.. PYTRATEACL RACPAACTCS HVERGCSVRC 43
zfNyx      ~~~~~MCFII NIA↓VYFLLLP PHALSLWACT RSCPPTCTCT Q.EKSCSVLC 44

huNYX 49   DRAGLLRVPA ELPCEAVSID LDRNGLRFLG ERAFGTLPSL RRLSLRHNNL  98
moNyx 44   DRAGLQRVPQ EFPCEAASID LDRNGLRILG ERAFGTLPSL RRLSLRHNNL  93
zfNyx 45   DHVNMMDLPK EFPCEASSIN LDKNSLKFLS ERAFGTLPSL KTLSLKYNNI  94

huNYX  99  SFITPGAFKG LPRLAELRLA HNGDLRYLHA RTFAALSRLR RLDLAACRLF 148
moNyx  94  SFITPGAFKG LPRLAELRLA HNGELRYLHV RTFAALGRLR RLDLAACRLF 143
zfNyx  95  SFITPGAFKG LPNLVELKMA HNEYIRYLHT RTFTALKRLV RLDLSDCNLF 144

huNYX 149  SVPERLLAEL PALRELAAFD NLFRRVPGAL RGLANLTHAH LERGRIEAVA 198
moNyx 144  SVPERLLAEL PALRELTAFD NLFRRVPGAL RGLANLTHAH FERSRIEAVA 193
zfNyx 145  NMPDRIFLEQ ITLKELLCFQ NNFRRVPGAL RGMENLTHVY LERNKIEAVA 194

huNYX 199  SSSLQGLRRL RSLSLQANRV RAVHAGAFGD CGVLEHLLLN DNLLAELPAD 248
moNyx 194  SGSLLGMRRL RSLSLQANRV RAVHAGAFGD CGALEDLLLN DNLLATLPAA 243
zfNyx 195  YNSLLGLTSL KYLNLQENRI NVIHDEAFKD LIRLENFYLN DNLLVDLPQQ 244


huNYX 248  AFRGLRRLRT LNLGGNALDR VARAWFADLA ELELLYLDRN SIAFVEEGAF 298
moNyx 244  AFRGLRRLRT LNLGGNALGS VARAWFSDLA ELELLYLDRN SITFVEEGAF 293
zfNyx 245  AFKGLSNLKM LNLGGNLLTN VSKTWFSDLV ELEVLYLDRN RLSYIEDGSF 294


huNYX 299  QNLSGLLALH LNGNRLTVLA WVAFQPGFFL GRLFLFRNPW CCDCRLEWLR 348
moNyx 294  QNLSGLLALH LNGNRLTVLS WAAFQPGFFL GRLFLFRNPW RCDCQLEWLR 343
zfNyx 295  ENLTSLITLH LNSNNLTSLP FSVFQPIYFI GRLYLFRNPW ECTCDLEWLR 344

huNYX 349  DWMEGSGRVT DVPCASPGSV AGLDLSQVTF GRSSDGLCVD PEELNLTTSS 398
moNyx 344  DWMEGSGRVA DVACASPGSV AGQDLSQVVF ERSSDGLCVD PDELNFTTSS 393
zfNyx 345  EWMESYKLVR DIPCASPSSV AGLDLSEVVF AH.LNSTCLD PPELNMTTSL 393

huNYX 399  PGPSPEPAAT TVSRFSSLLS KLLAPRVPVE EAANTTGGLA NASLSDSLSS 448
moNyx 394  PGPSPEPVAT TVSRFSSLLS KLLAPRAPVE EVANTTWELV NVSLNDSFRS 443
zfNyx 395  P.....DYPT VENKFNSLIS KLLQQELR.D EMVNITDSLR NGTQQDPAES 437

huNYX 449  RGVGGAGRQP WFLLASCLLP SVAQHVVFGL QMD~~~~~ 481
moNyx 444  HAVMVFCYKA TFLFTSCVLL SLAQYVVVGL QRE~~~~~ 476
zfNyx 439  Q...VSSAHG LFGASQTVFL LV...VLFQA QFDSINAS 469
```

FIG. 1. Amino acid sequence comparison of the zebrafish Nyx and its human and mouse orthologs. The N-terminal signal peptides and the C-terminal predicted GPI anchors predicted by the version of Expasy-tools are boxed. The arrows indicate the exon 2 – exon 3 boundaries in the three species. Amino acids in bold represent the peptide against which the zebrafish-specific anti-Nyx antibody was designed.

splice site which was found in human and mouse between amino acid residues 12 and 13 is different in zebrafish, as shown by alignment of the cDNA and the genomic sequence data. However, the overall exon structure is similar. The zf *nyx* gene consists of three exons, and the ORF is confined to exons 2 and 3, analogous to the human and mouse gene. Although the exon sizes are similar in all three species, intron 2 is much smaller in the zebrafish gene than in the mouse and human (2 kb compared with 18 and 25 kb, respectively).

The zebrafish gene encodes 469 amino acid residues, whereas 481 and 476 amino acids were predicted for human and mouse, respectively (Bech-Hansen *et al*., 2000; Pusch *et al*., 2000, 2003). Computational predictions of the zf Nyx revealed a signal peptide, an LRR core and a GPI anchor. These motifs were also assumed in human and mouse except for the GPI anchor, which was only predicted for the human gene (Bech-Hansen *et al*., 2000; Pusch *et al*., 2000, 2003). However, *in vitro* studies showed that both the human and the mouse Nyx proteins are cell surface proteins (Zeitz *et al*., 2003; O'Connor *et al*., 2005).

Nyx is expressed in the inner nuclear layer

Several studies investigated the distribution of *NYX* mRNA in the retina of mouse and human. The *Nyx* transcript was either detected in the cells within the INL (Gregg *et al*., 2003) or in the INL and ganglion cell layer (GCL) (Pesch *et al*., 2003) of the mouse retina. In the human retina *NYX* was reported to be expressed in the cell bodies of the photoreceptor cell layer, the INL and GCL (Bech-Hansen *et al*., 2000; Pesch *et al*., 2003).

In order to address this question in another vertebrate species, we determined the expression pattern in the retina of the zebrafish.

We used four developmental stages (2–5 dpf) to study the transcription pattern of *nyx* during development in the retina by RNA *in situ* hybridization. Weak expression was first observed at 3 dpf in central regions of the inner nuclear cell layer. At later stages the localization of zf *nyx* expands into more peripheral regions where newborn cells are added (Fig. 2C). Compared with other retinal genes, the expression was very low, as indicated by the time course of the coloring reaction (data not shown). At all stages no transcripts were detected in either the photoreceptor or the ganglion cell layer. No signal was detected by using the sense probe (Fig. 2D).

Cellular organization of the retina in the nyx morphants are not affected

In order to determine the function of Nyx *in vivo*, we performed a loss-of-function study using antisense morpholino-modified oligonucleo-

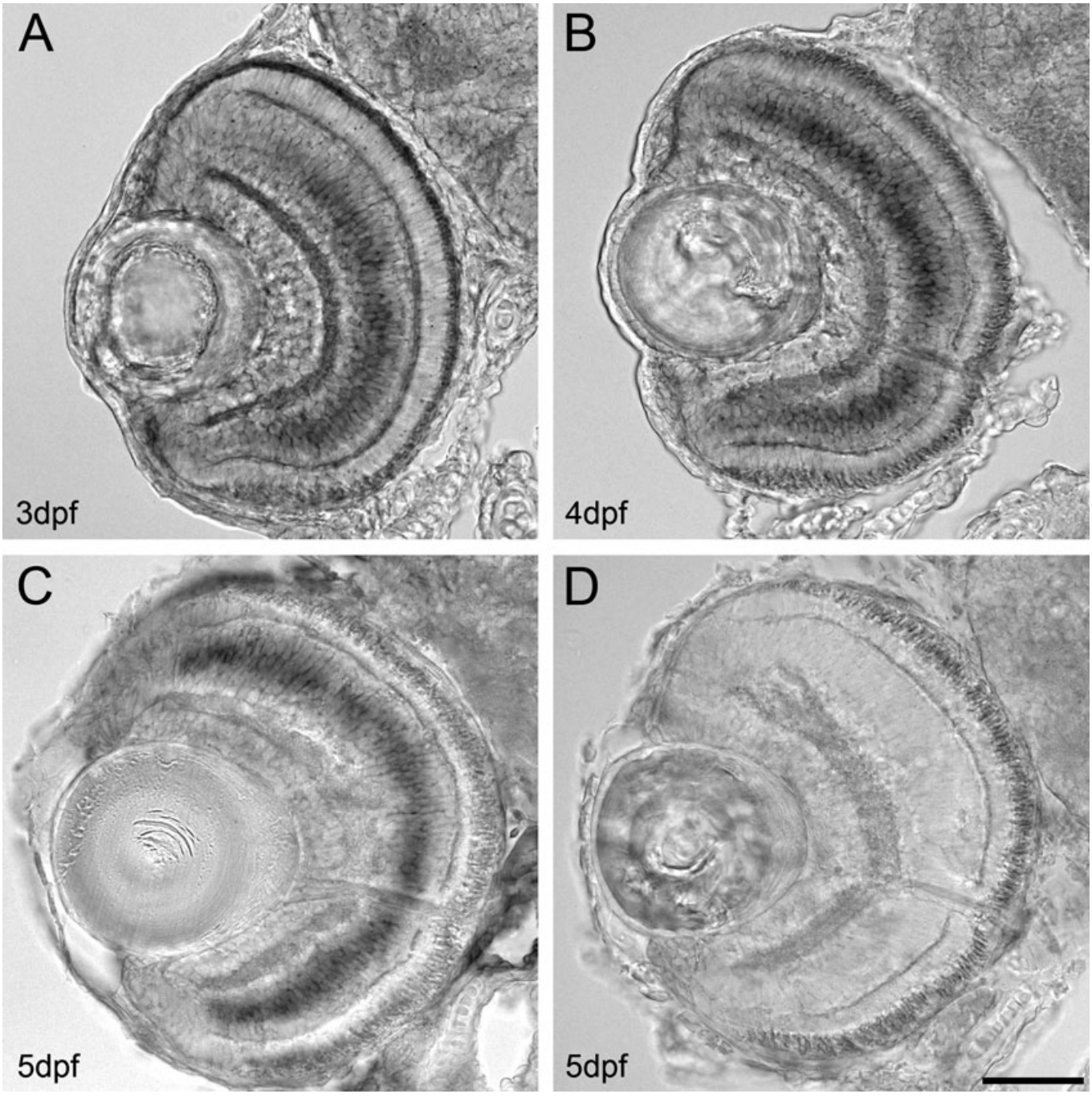

FIG. 2. *nyx* localization in the larval zebrafish retina. Transverse sections of whole mount *in situ* hybridization through the developing zebrafish retina between 3 and 5 days post-fertilization (dpf) by using a Dig-labeled *nyx* antisense probe are shown. The *nyx* mRNA is expressed in cells of the mid row of the inner nuclear layer (A, B and C). (A) *nyx* is expressed in the central part of the inner nuclear layer as early as 3 dpf. (B and C) Expression spreads from centrally to the periphery of the inner nuclear layer. (D) *nyx* sense control in the zebrafish retina. Scale bar, 50 μm.

tides (MO) (Nasevicius & Ekker, 2000). The antisense morpholino nucleotide was designed against the translation initiation site of the *nyx* gene. As a control, an MO without any targeted sequence and significant biological activity was used. The larvae were injected with *nyxMO* and *controlMO* at the one- to four-cell stages. Morpholino-injected larvae hatched normally and did not display any obvious morphological defects.

We first addressed the question of whether the absence of Nyx in the respective *nyx* morphants at 4 dpf affects the cellular organization or the synaptic connection of the retina. The zebrafish retina is fully developed at 60 h post-fertilization – all retinal cell types (photoreceptors, bipolar, horizontal, amacrine, ganglion and Mueller glia cells) are present at this stage (Schmitt & Dowling, 1999). The classical ultrastructural components at the cone terminal, namely cone synaptic ribbons, bipolar cell dendrites and horizontal cell spinules, reach morphological maturity within the first 5 days of development (Biehlmaier *et al*., 2003). Synaptic connection between photoreceptors and bipolar as well as horizontal cells in the outer plexiform layer, and between ganglion and bipolar as well as amacrine cells in the inner plexiform layer, are also formed. We investigated the morphology of the retina by preparing standard histological sections through the eye of positive tested morpholino-treated larvae. We found no evidence for morphological alterations in the retina of *nyx* morphants (Fig. 3A) compared with control morphants (Fig. 3B). Our results clearly demonstrate that the retinal layering and all major cell types are not affected in the *nyxMO*-injected larvae. This result is supported by preliminary ultrastructural data that found no evidence for structural changes (data not shown).

Distribution of Nyx protein in the developing zebrafish retina

To study the localization of the nyctalopin protein in the larval zebrafish retina, we raised a zebrafish-specific nyctalopin polyclonal peptide antibody. The epitope was designed using the zebrafish sequence and directed against LRRs. To ensure the specificity of the anti-Nyx antibody directed against a peptide of the C-terminal zf NYX protein, flag-tagged zf *nyx* constructs were transiently expressed in COS-7 cells. Anti-Nyx and anti-flag antibodies both stained only cells expressing the Nyx-flag-tagged protein (Fig. 4) while non-expressing cells were free from any staining. The intracellular honeycomb-like localization of the zf Nyx protein is similar to the human and mouse (Zeitz *et al*., 2003).

To identify the localization of the Nyx protein in the retina, we double labeled 5-dpf larvae for Nyx and SV2, a presynaptic marker (Buckley & Kelly, 1985; Feany *et al*., 1992) (Fig. 5A). Nyx is localized in both synaptic layers of the zebrafish retina (Fig. 5A). We observed no co-localization between Nyx and SV2, suggesting a postsynaptic localization of Nyx (Fig. 5C). To confirm additionally the postsynaptic localization of Nyx, we double labeled 5-dpf larvae with Nyx and PSD-95, another presynaptic marker (Koulen *et al*., 1998). The deconvolved image of the labeling in the OPL clearly shows that Nyx and PSD-95 do not co-localize (Fig. 6A). Invagination of Nyx-labeled second-order neuron dendrites into PSD-95-labeled cone pedicles can be clearly identified, confirming the postsynaptic localization of Nyx (Fig. 6B and C). A close examination of the Nyx staining (Fig. 5A) revealed a specific, somewhat punctual labeling for the nyctalopin protein, suggesting that it might be present in specific clusters, especially throughout the IPL.

Additionally, we examined the retinal localization of nyctalopin in wild-type and *nyxMO*-injected larvae at 4 dpf (Fig. 7). In the wild-type, we found the same situation as described above, strong pre- (SV2) and postsynaptic (Nyx) labeling of the synaptic layers (Fig. 7C). As expected, the Nyx labeling was virtually gone in the *nyx* morphants (Fig. 7D and F). Thus, the postsynaptic localization of nyctalopin could no longer be found in the merged picture (Fig. 7F) of the *nyxMO*-treated larvae.

Impairment of b-wave in the ERG of Nyx-deficient larvae

The ERG can be reliably measured in zebrafish larvae (Branchek, 1984; Makhankov *et al*., 2004). The ERG response to a short light flash consists of two major components: a hyperpolarizing, often very

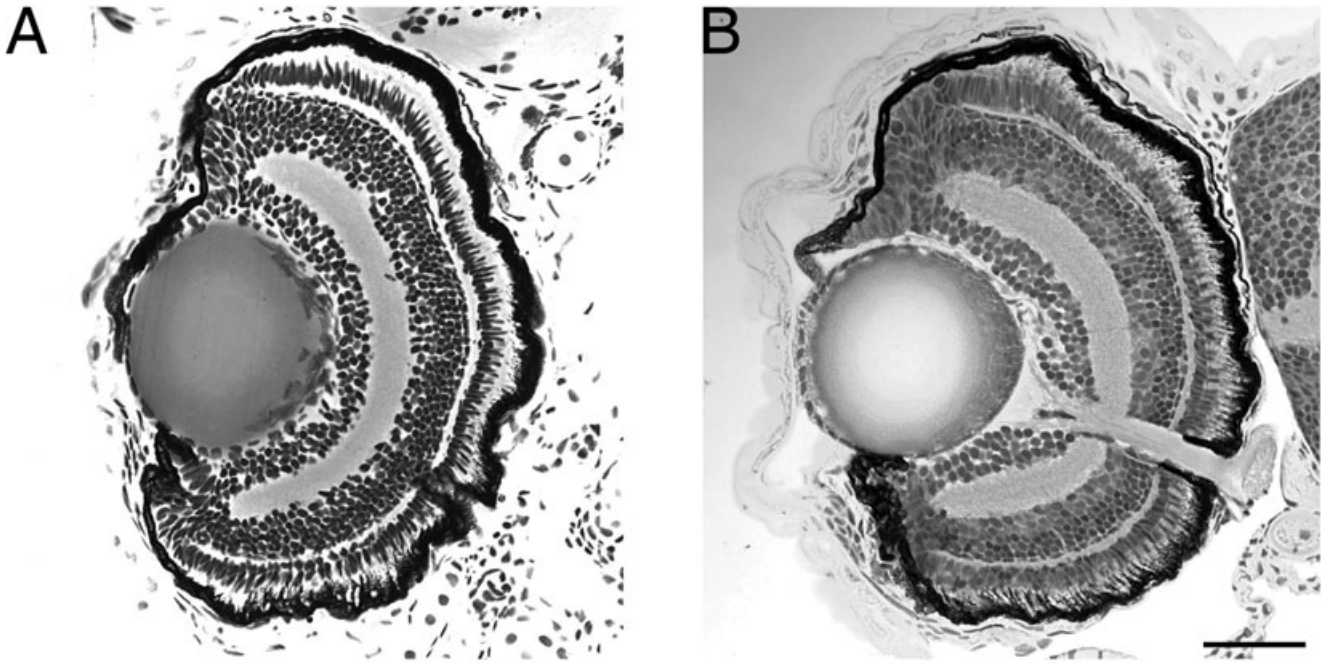

FIG. 3. Eye morphology of the retina of *controlMO* and *nyxMO*-injected larvae. Eye morphology of 4 dpf control (A) and *nyxMO*-injected larvae (B). In transverse sections through the eyes no morphological defect in the retina of *nyxMo*-treated larvae is observed. Scale bar, 50 μm.

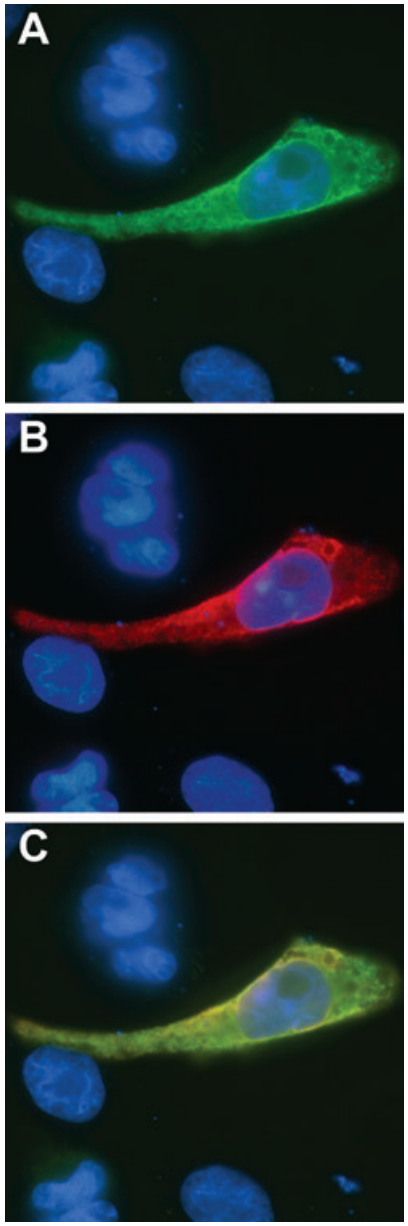

FIG. 4. Specificity of the zebrafish anti-Nyx antibody. The staining of the anti-flag antibody (A) perfectly overlaps with the staining of the anti-Nyx antibody targeted against the C-terminal part of the zebrafish Nyx protein (B), intracellularly in a honey-comb pattern (C).

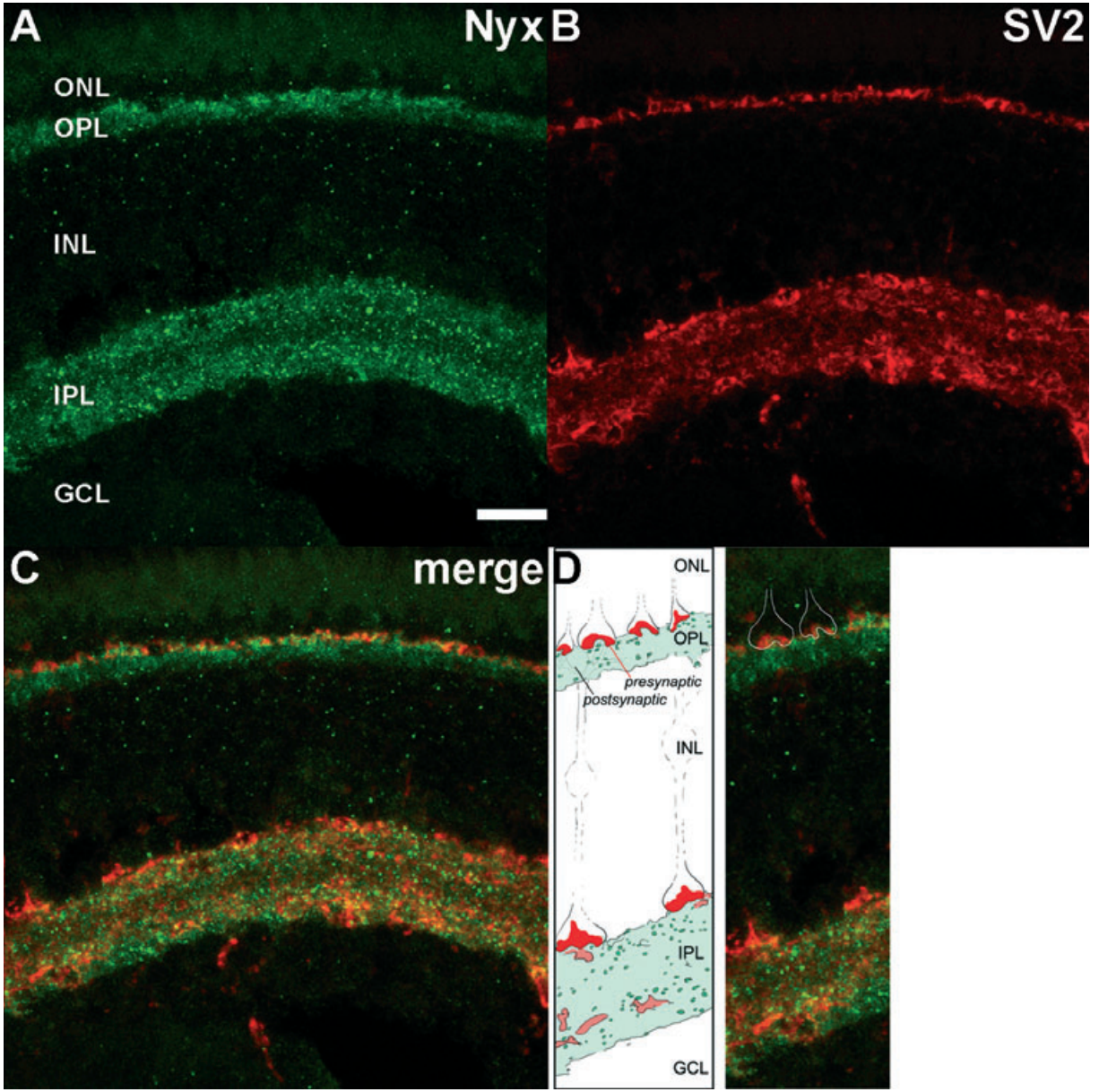

FIG. 5. Confocal image of Nyx (green) and SV2 (red) double immunostaining in -dpf wild-type larvae. Strong Nyx labeling is visible in the synaptic layers (A). In the merged image (C) the postsynaptic localization of the Nyx labeling is clear, as the SV2 (B) labeling is localized in presynaptic structures. (D) A schematic drawing depicting Nyx localization in the retina. Scale bar, 10 μm.

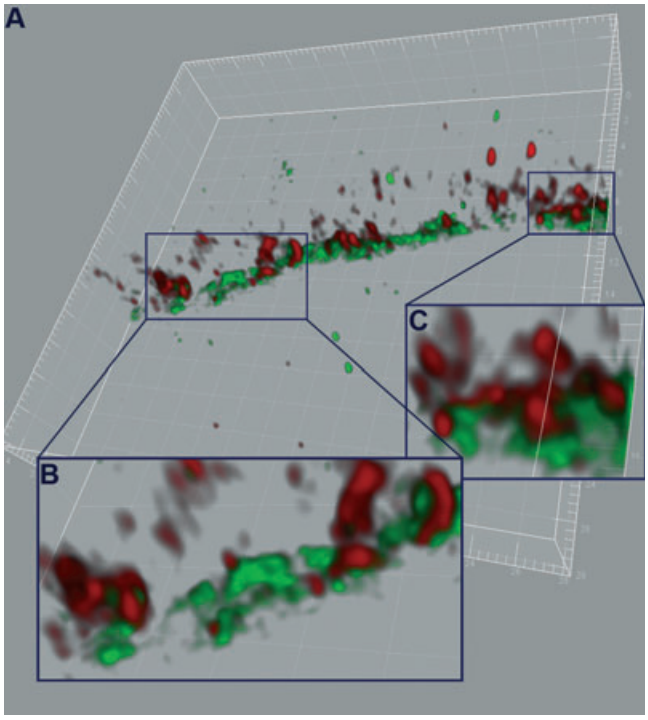

FIG. 6. Deconvolved confocal reconstruction of Nyx (green) and PSD95 (red) double immunostaining in the outer plexiform layer of 5-dpf wild-type larvae. The presynaptical localization of the PSD-95 labeling and the postsynaptical labeling of Nyx can be clearly identified (A), especially in the close-ups of single photoreceptor pedicles of the outer plexiform layer (B and C). Grid spacing, 2 μm.

short a-wave and a somewhat delayed depolarizing b-wave. The a-wave reflects photoreceptor activity, whereas the b-wave represents ON-bipolar cell activity (Dowling, 1987). We studied the ERGs of 4- and 5-dpf larvae treated with two different MO concentrations (approximatelly 30 ng and 15 ng) and compared them with the responses of control MO-treated ($n = 8$) and those of wild-type larvae ($n = 5$). Control morphants exhibited ERG (Fig. 8A) that were undistinguishable from those of wild-type larvae (not shown). The typical ERG of the 30-ng MO group misses the b-wave (Fig. 7B). In a few larvae, weak b-wave-like depolarizations were present during the first series of flashes and sometimes low-frequency oscillations were visible. In six larvae, no ERG responses could be recorded. The responses of the 15-ng MO group were more variable, and a b-wave contribution was more frequently observed. Therefore, nyx morpholino injection suppresses b-wave development in a concentration-dependent fashion.

Our experience with wild-type larvae is that OFF responses (d-waves), i.e. short depolarizing deflections after a long stimulus, cannot be elicited consistently with our set-up. We therefore concluded that the d-wave is not a reliable tool for monitoring OFF bipolar cell activity and we made no attempt to study the OFF response in nyx morphants.

Visually mediated behavior in Nyx-depleted larvae

In mGluR6-null mice, a deficit in ON bipolar cell pathway in the retina is associated with visual dysfunction. Mutant mice respond to light, but are severely impaired in optokinetic behavior, indicating a deficit in contrast sensitivity (Iwakabe *et al*., 1997). In order to test the impact

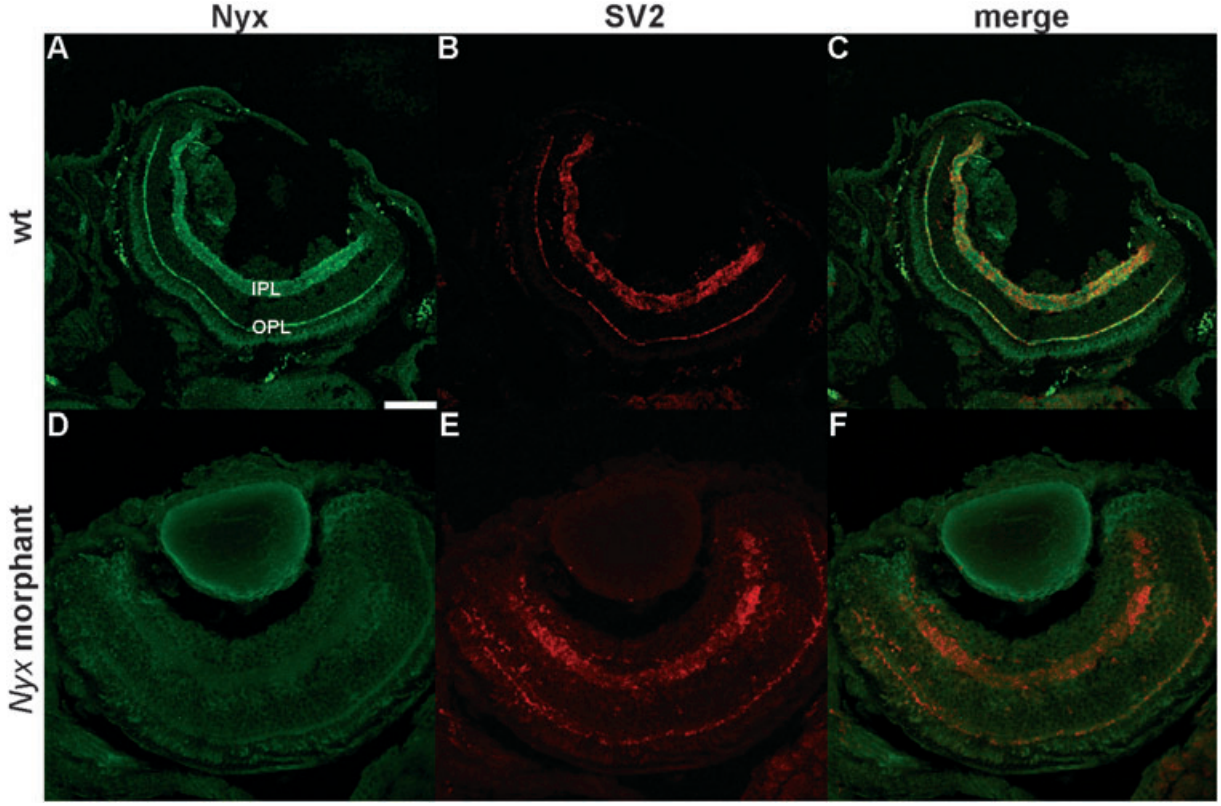

FIG. 7. Confocal images of Nyx (green) and SV2 (red) double immunostaining in 4-dpf wild-type and *nyxMO*-treated larvae. In the wild-type a clear labeling is visible for both presynaptic SV2 (B) and postsynaptic Nyx labeling (A), and merged (C). By contrast, labeling of both proteins is clearly reduced in the morpholino-injected larvae (Nyx, D; SV2, E; merge, F). Scale bar, 50 μm.

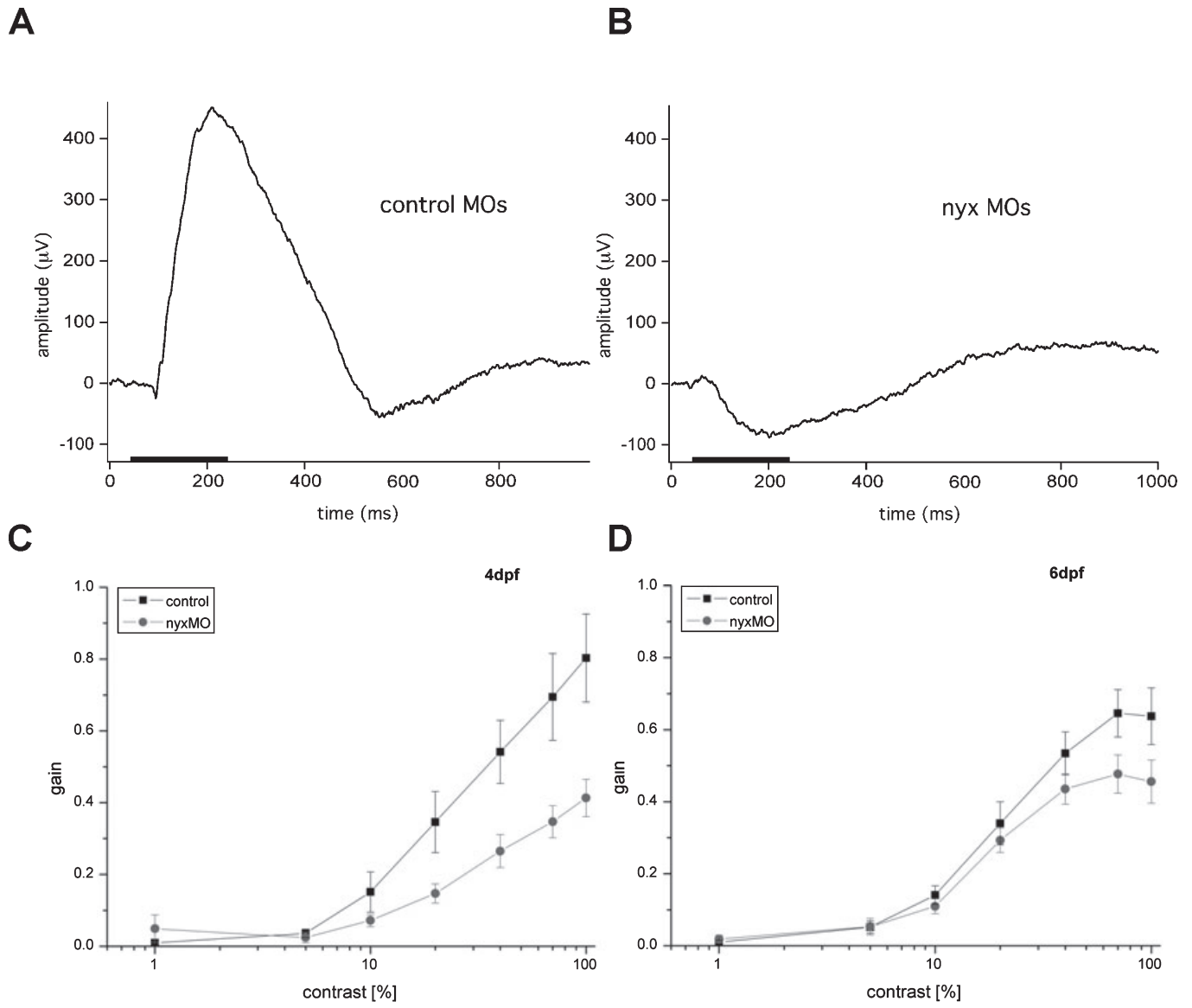

FIG. 8. Electroretinogram (ERG) recordings (A and B) and behavioral analysis (C and D) of *nyx* morphants. Averaged ERG traces of both *controlMO*- (A) and *nyxMO*- (B) treated larvae at 4 dpf. Typical ERG of control larvae (A) consisting of a- and b-waves. By contrast typical ERGs of *nyxMO*-treated larvae (B) show only an a-wave. Horizontal bars indicate 200-ms light stimuli. (C and D) Behavioural analysis of the optokinetic response reveals a reduction in contrast sensitivity at 4 dpf in *nyx* morphants (C). At 6 dpf contrast sensitivity is similar to control larvae (D). Error bars indicate standard error of the mean derived from the bootstrap sampling distribution.

of Nyx deficiency on visual performance, we used a similar behavioral paradigm, the optokinetic response (OKR).

Contrast sensitivity of both *nyx* and control morphants at different stages (4 and 6 dpf) was analysed by measuring the OKR triggered by grating stimuli with varying contrast (5–97%). Contrast sensitivity of *nyxMO*-treated larvae was reduced compared with control larvae (bootstrap resampling test, $P < 0.05$). This reduction in contrast sensitivity is most apparent at 4 dpf (Fig. 8C), becoming less pronounced at 6 dpf (Fig. 8D). This is probably due to a recovery in Nyx protein levels, as morphants presumably become more diluted with increasing age, and thereby diminishing their blocking effect on protein synthesis.

These results show that in *nyxMO*-treated larvae contrast sensitivity is impaired (Fig. 8C and D). However, no difference in spatial resolution between *nyx* and control morphants was found (data not shown).

Discussion

Nyctalopin, encoded by the *Nyx* gene, has been implicated in the function of the photoreceptor synapse, selectively affecting the ON-pathway (Bech-Hansen *et al.*, 2000). Mutations in the respective gene in humans are associated with congential stationary nightblindness type 1 (CSNB1), assuming a defective synaptic transmission in the rod photoreceptor pathway. The human retina is functionally cone-dominant, with most of our daily vision completely supported by cone photoreceptors. The cone pathway in CSNB1 patients is variably affected, but to a lesser degree than the rod pathway (Lachapelle *et al.*, 1983; Miyake *et al.*, 1986; Bech-Hansen *et al.*, 2000). In order to analyse the function of nyctalopin in a cone-dominant retina, we isolated the ortholog in zebrafish and determined its expression in the developing zebrafish retina. Expression starts in the inner retina at 3 dpf, concomitant with synaptic maturation

(Biehlmaier *et al*., 2003). Consistent with data in other organisms expression levels are low. We raised a polyclonal antibody against zebrafish nyctalopin and localized the protein at a presumably postsynaptic position opposite to the presynapse in both synaptic layers of the retina. Three-dimensional reconstructions of Nyx/PSD-95 double-labelings strengthen the hypothesis of a postsynaptic localization of Nyctalopin. However, the ultimate proof of a postsynaptic localization has to await co-localization studies with a postsynaptic marker, compatible with Nyx staining. Hence, we conclude that the protein is produced in the INL – presumably in ON-bipolar cells – and ganglion cells. This is consistent with data from the mouse (Gregg *et al*., 2003; Pesch *et al*., 2003; Ren *et al*., 2004). Similar to mouse but in contrast to studies using human retinas (Bech-Hansen *et al*., 2000), we did not detect any nyctalopin transcript or protein in photoreceptors. Additionally, we did not observe *nyx* transcript in ganglion cells. This might be due to the fact that *nyx* expression is below detection level in the zebrafish GCL.

The larval retina can be regarded as cone-dominant, allowing the genetic analysis of vertebrate cone vision. Few nascent rods are formed at early stages of zebrafish retinal development (Branchek & Bremiller, 1984; Raymond *et al*., 1995; Schmitt & Dowling, 1999), and rod-driven responses can only be recorded at stages older than 15 dpf (Clark, 1981; Bilotta *et al*., 2001). Most of the human retinal disorders are studied using the rod-dominated mouse model, so the cone-dominant zebrafish is an important addition to the existing animal model of human retinal diseases.

To investigate the function of nyctalopin and its contribution to cone vision we knocked down nyctalopin protein by injection of morpholino antisense nucleotides targeted against the translational start site. Although most studies show that the knock-down efficiency is high during the first 50 h of development (e.g. Nasevicius & Ekker, 2000), recent studies indicate that morpholino activity can be long-lasting, allowing the generation of functional knock-downs of up to 7 dpf (Sollner *et al*., 2004; Rinner *et al*., 2005a; Seiler *et al*., 2005)

We verified the effectiveness of the nyctalopin knock-down at 4 dpf by virtue of loss of immunoreactivity on retinal sections and the loss of the b-wave in ERGs.

Depleting the retina of nyctalopin has no effect on retinal morphology; all major cell types develop and retinal layering is unaffected. Similar to effects on the human and mouse visual system, all observed effects of nyctalopin depletion in the zebrafish retina are functional and not structural in nature.

Nyctalopin-depleted zebrafish larvae display the characteristic Schubert–Bornschein-type ERG, characterized by a reduced or absent b-wave. Because the b-wave reflects activity of ON-bipolar cells, such a response is indicative of defective neurotransmission between photoreceptors and downstream ON-bipolar cells. Light perception by photoreceptors is unaffected, as evidenced by the prominent a-wave reflecting photoreceptor activation. Similar recordings are obtained from CSNB1 patients with mutations in the *NYX* gene (Bech-Hansen *et al*., 2000; Pusch *et al*., 2000) or from patients with mutations in the *GRM6* gene encoding the metabotropic glutamate receptor 6 (mGluR6) (Dryja *et al*., 2005; Zeitz, 2005). The Schubert–Bornschein-type ERG shows a normal OFF response. As we cannot reliably measure the OFF response in zebrafish larvae, we can reach no conclusion about the function of the OFF response in morphant larvae. Using long (1 s) flashes with MO morphants missing the b-wave, we do observe a depolarizing wave after light off. But unlike a proper d-wave the response is much delayed and slow (data not shown); it might indicate an OFF response of the photoreceptors.

Therefore, nyctalopin deficiency induces a phenotype similar to that of CSNB1 in a cone-dominant animal model of this disease. Another phenotype of unknown origin in CSNB1 is myopia. Zebrafish larvae are emmotropic at about 3 dpf (Easter & Nicola, 1996) and there is little evidence for accommodation. Therefore, this aspect of the human disease cannot be investigated in zebrafish larvae.

The *nob* (no b-wave) mouse is mutated in the *Nyx* gene and also displays – as the name implies – this characteristic electroretinogram (Gregg *et al*., 2003). Gregg *et al*. rescued the ERG phenotype by transgene expression of Nyx in bipolar cells of Nyx-mutated *nob* mice, confirming the role of Nyx in synaptic transmission between photoreceptors and bipolar cells (Gregg *et al*., 2005). All these data lend support to the hypothesis that nyctalopin functions postsynaptic to the photorepceptor synapse and is involved in signal transmission to ON bipolar cells.

Although the functional significance of nyctalopin for ON-bipolar cell function is evident, little is known about its function in ganglion cells. The protein is located postsynaptically in both sublaminae of the inner plexiform layer, indicating that it is expressed in both ON- and OFF-ganglion cells. Because these synapses are not accessible to functional studies by electroretinography, clarification of the role of nyctalopin in synaptic transmission in the inner plexiform layer must await more sophisticated electrophysiological experiments. However, it is clear that synaptic transmission cannot be completely disrupted, as visual behavior is affected but not abolished. We assessed the effect of nyctalopin knockdown on overall visual performance by recording optokinetic reflexes. Deficiency of Nyx in morpholino-treated larvae leads to a modest reduction in contrast sensitivity. Therefore, a block of the ON-pathway through the retina still allows fairly intact vision. Blocking the ON-channel pharmacologically by applying the glutamate agonist amino-phosphonobutyrate (Schiller *et al*., 1986) or genetically in the mGluR6 knockout mouse similarly leads to visual deficits but not to a complete loss of vision (Iwakabe *et al*., 1997). This is consistent with the notion that sufficient information for motion detection can be carried by the OFF-channel or that the ON-channel is not completely blocked in these experiments.

What might be the role of nyctalopin in retinal synapse function? The structure of the protein containing 11 LRRs suggests a function of this protein in protein–protein interaction. Interestingly no interaction partner has been identified so far.

We and others have demonstrated the cell surface localization of nyctalopin (Zeitz *et al*., 2003; O'Connor *et al*., 2005; this study), consistent with a potential role in cell adhesion. In *Drosophila* two members of the small leucine-rich repeat proteoglycan family play pivotal roles as cell adhesion molecules in neuronal development. Chaoptin, which is linked to the extracellular surface of the plasma membrane by a GPI anchor, belongs to the cell adhesion molecules and is required for photoreceptor cell morphogenesis (Krantz & Zipursky, 1990). Connectin is located at some neuromuscular synaptic sites during synaptic formation and is implicated as a repulsive factor during growth cone guidance and synapse formation (Nose *et al*., 1994). Similar to chaoptin and connectin, nyctalopin might have a role as an adhesion molecule and could be involved in support formation of synaptic connection between photoreceptor and second-order neurons during development.

In summary, we have demonstrated that Nyx is postsynaptically located in the retina and plays a crucial role in the cone visual pathway. Additionally, the zebrafish model, owing to its visual system properties combined with superb genetics, offers the opportunity to create animal models of ocular diseases, as exemplified here for CSNB1.

Acknowledgements

We dedicate this paper to the memory to Joe Bilotta, a pioneer in zebrafish electroretinography. We have unexpectedly lost a dear colleague and friend. We thank David Belet for technical assistance, and Urs Ziegler for helping O.B. with deconvolution. We also thank Drs Martin Schwab, Dana Dodd and Oliver Rinner for helpful discussions and reading of the manuscript. This work was supported by the Swiss National Science Foundation (SNF), the Velux Foundation, the EMBO Young Investigator Program (S.C.F.N.), Hartmann Müller Foundation and ETH internal grants. During part of the study S.C.F.N. was funded by the SNF as an SNF Förderungsprofessor.

Abbreviations

CSNB, congenital stationary night blindness; dpf, days post-fertilization; ERG, electroretinogram; GCL, ganglion cell layer; GPI, glycosylphosphatidylinositol; INL, inner nuclear layer; LRRs, leucine-rich repeats; mGluR, metabotropic glutamate receptor; MO, morpholino; OKR, optokinetic response; ORF, open reading frame; PSD-95, mouse anti-postsynaptic density 95 kDa; SV2, mouse anti-synaptic vesicle 2.

References

Bech-Hansen, N.T., Naylor, M.J., Maybaum, T.A., Sparkes, R.L., Koop, B., Birch, D.G., Bergen, A.A., Prinsen, C.F., Polomeno, R.C., Gal, A., Drack, A.V., Musarella, M.A., Jacobson, S.G., Young, R.S. & Weleber, R.G. (2000) Mutations in NYX, encoding the leucine-rich proteoglycan nyctalopin, cause X-linked complete congenital stationary night blindness. *Nat. Genet.*, **26**, 319–323.

Biehlmaier, O., Neuhauss, S.C. & Kohler, K. (2003) Synaptic plasticity and functionality at the cone terminal of the developing zebrafish retina. *J. Neurobiol.*, **56**, 222–236.

Bilotta, J., Saszik, S. & Sutherland, S.E. (2001) Rod contributions to the electroretinogram of the dark-adapted developing zebrafish. *Dev. Dyn.*, **222**, 564–570.

Branchek, T. (1984) The development of photoreceptors in the zebrafish, *Brachydanio rerio*. II. Function. *J. Comp. Neurol.*, **224**, 116–122.

Branchek, T. & Bremiller, R. (1984) The development of photoreceptors in the zebrafish, *Brachydanio rerio*. I. Structure. *J. Comp. Neurol.*, **224**, 107–115.

Brand, M.G.M. & Nüsslein-Volhard, C.H. (2002) Keeping and raising zebrafish. In Nusslein-Volhard, C. & Dahm, R. (Eds), *Zebrafish, Practical Approach Series*. Oxford University Press, Oxford, pp. 7–37.

Buckley, K. & Kelly, R.B. (1985) Identification of a transmembrane glycoprotein specific for secretory vesicles of neural and endocrine cells. *J. Cell Biol.*, **100**, 1284–1294.

Clark, D.T. (1981) Visual responses in the developing zebrafish (*Brachydanio rerio*). PhD Thesis, University of Oregon Press, Eugene, OR.

Dowling, J.E. (1987) *The Retina: an Approachable Part of the Brain.* Harvard University Press, Cambridge, MA.

Dryja, T.P., McGee, T.L., Berson, E.L., Fishman, G.A., Sandberg, M.A., Alexander, K.R., Derlacki, D.J. & Rajagopalan, A.S. (2005) Night blindness and abnormal cone electroretinogram ON responses in patients with mutations in the GRM6 gene encoding mGluR6. *Proc. Natl Acad. Sci. USA*, **102**, 4884–4889.

Easter, S.S. Jr & Nicola, G.N. (1996) The development of vision in the zebrafish (*Danio rerio*). *Dev. Biol.*, **180**, 646–663.

Feany, M.B., Lee, S., Edwards, R.H. & Buckley, K.M. (1992) The synaptic vesicle protein SV2 is a novel type of transmembrane transporter. *Cell*, **70**, 861–867.

Grant, G.B. & Dowling, J.E. (1995) A glutamate-activated chloride current in cone-driven ON bipolar cells of the white perch retina. *J. Neurosci.*, **15**, 3852–3862.

Gregg, R.G., McCall, M. & Peachey, N.S. (2005) Bipolar specific expression of nyctalopin fusion gene rescues No-B wave phenotype in Nob mice. *Invest. Ophthalmol. Vis. Sci.*, **46**, E-Abstract 3554.

Gregg, R.G., Mukhopadhyay, S., Candille, S.I., Ball, S.L., Pardue, M.T., McCall, M.A. & Peachey, N.S. (2003) Identification of the gene and the mutation responsible for the mouse nob phenotype. *Invest. Ophthalmol. Vis. Sci.*, **44**, 378–384.

Iwakabe, H., Katsuura, G., Ishibashi, C. & Nakanishi, S. (1997) Impairment of pupillary responses and optokinetic nystagmus in the mGluR6-deficient mouse. *Neuropharmacology*, **36**, 135–143.

Kobe, B. & Deisenhofer, J. (1994) The leucine-rich repeat: a versatile binding motif. *Trends Biochem. Sci.*, **19**, 415–421.

Koulen, P., Fletcher, E.L., Craven, S.E., Bredt, D.S. & Wässle, H. (1998) Immunocytochemical localization of the postsynaptic density protein PSD-95 in the mammalian retina. *J. Neurosci.*, **18**, 10136–10149.

Krantz, D.E. & Zipursky, S.L. (1990) Drosophila chaoptin, a member of the leucine-rich repeat family, is a photoreceptor cell-specific adhesion molecule. *EMBO J.*, **9**, 1969–1977.

Lachapelle, P., Little, J.M. & Polomeno, R.C. (1983) The photopic electroretinogram in congenital stationary night blindness with myopia. *Invest. Ophthalmol. Vis. Sci.*, **24**, 442–450.

Makhankov, Y.V., Rinner, O. & Neuhauss, S.C. (2004) An inexpensive device for non-invasive electroretinography in small aquatic vertebrates. *J. Neurosci. Methods*, **135**, 205–210.

Miyake, Y., Yagasaki, K., Horiguchi, M., Kawase, Y. & Kanda, T. (1986) Congenital stationary night blindness with negative electroretinogram. A new classification. *Arch. Ophthalmol.*, **104**, 1013–1020.

Nasevicius, A. & Ekker, S.C. (2000) Effective targeted gene 'knockdown' in zebrafish [In Process Citation]. *Nat. Genet.*, **26**, 216–220.

Nose, A., Takeichi, M. & Goodman, C.S. (1994) Ectopic expression of connectin reveals a repulsive function during growth cone guidance and synapse formation. *Neuron*, **13**, 525–539.

O'Connor, E., Eisenhaber, B., Dalley, J., Wang, T., Missen, C., Bulleid, N., Bishop, P.N. & Trump, D. (2005) Species specific membrane anchoring of nyctalopin, a small leucine-rich repeat protein. *Hum. Mol. Genet.*, **14**, 1877–1887.

Pardue, M.T., McCall, M.A., LaVail, M.M., Gregg, R.G. & Peachey, N.S. (1998) A naturally occurring mouse model of X-linked congenital stationary night blindness. *Invest. Ophthalmol. Vis. Sci.*, **39**, 2443–2449.

Pesch, K., Zeitz, C., Fries, J.E., Munscher, S., Pusch, C.M., Kohler, K., Berger, W. & Wissinger, B. (2003) Isolation of the mouse nyctalopin gene nyx and expression studies in mouse and rat retina. *Invest. Ophthalmol. Vis. Sci.*, **44**, 2260–2266.

Pusch, C.M., Zeitz, C., Brandau, O., Pesch, K., Achatz, H., Feil, S., Scharfe, C., Maurer, J., Jacobi, F.K., Pinckers, A., Andreasson, S., Hardcastle, A., Wissinger, B., Berger, W. & Meindl, A. (2000) The complete form of X-linked congenital stationary night blindness is caused by mutations in a gene encoding a leucine-rich repeat protein. *Nat. Genet.*, **26**, 324–327.

Raymond, P.A., Barthel, L.K. & Curran, G.A. (1995) Developmental patterning of rod and cone photoreceptors in embryonic zebrafish. *J. Comp. Neurol.*, **359**, 537–550.

Ren, C., Akileswaran, L., Wang, G., Gregg, R. & Morgans, C.W. (2004) Nyctalopin in the mammalian retina. *Invest. Ophthalmol. Vis. Sci.*, **45**, E-Abstract 5354.

Rinner, O., Makhankov, Y.V., Biehlmaier, O. & Neuhauss, S.C. (2005a) Knockdown of cone-specific kinase GRK7 in larval zebrafish leads to impaired cone response recovery and delayed dark adaptation. *Neuron*, **47**, 231–242.

Rinner, O., Rick, J.M. & Neuhauss, S.C. (2005b) Contrast sensitivity, spatial and temporal tuning of the larval zebrafish optokinetic response. *Invest. Ophthalmol. Vis. Sci.*, **46**, 137–142.

Rodieck, R.W. (1998) *The First Steps in Seeing*. Sinauer, Sunderland, Massachusetts.

Schiller, P.H., Sandell, J.H. & Maunsell, J.H. (1986) Functions of the ON and OFF channels of the visual system. *Nature*, **322**, 824–825.

Schmitt, E.A. & Dowling, J.E. (1999) Early retinal development in the zebrafish, *Danio rerio*: light and electron microscopic analyses. *J. Comp. Neurol.*, **404**, 515–536.

Seiler, C., Finger-Baier, K.C., Rinner, O., Makhankov, Y.V., Schwarz, H., Neuhauss, S.C. & Nicolson, T. (2005) Duplicated genes with split functions: independent roles of protocadherin15 orthologues in zebrafish hearing and vision. *Development*, **132**, 615–623.

Sollner, C., Rauch, G.J., Siemens, J., Geisler, R., Schuster, S.C., Muller, U. & Nicolson, T. (2004) Mutations in cadherin 23 affect tip links in zebrafish sensory hair cells. *Nature*, **428**, 955–959.

Thisse, C., Thisse, B., Schilling, T.F. & Postlethwait, J.H. (1993) Structure of the zebrafish snail1 gene and its expression in wild-type, spadetail and no tail mutant embryos. *Development*, **119**, 1203–1215.

Wong, K.Y., Adolph, A.R. & Dowling, J.E. (2005) Retinal bipolar cell input mechanisms in giant danio. I. Electroretinographic analysis. *J. Neurophysiol.*, **93**, 84–93.

Zeitz, C. (2005) Mutations in GRM6 cause autosomal recessive congenital stationary night blindness with a distinctive scotopic 15 Hz flicker electroretinogram (ERG). *Invest. Ophthalmol. Vis. Sci.*, **46**, 4328–4335.

Zeitz, C., Scherthan, H., Freier, S., Feil, S., Suckow, V., Schweiger, S. & Berger, W. (2003) NYX (nyctalopin on chromosome X), the gene mutated in congenital stationary night blindness, encodes a cell surface protein. *Invest. Ophthalmol. Vis. Sci.*, **44**, 4184–4191.